PHYSICAL REVIEW B **91**, 235302 (2015)

Time-dependent stochastic Bethe-Salpeter approach

Eran Rabani
Department of Chemistry, University of California and Lawrence Berkeley National Laboratory, Berkeley, California 94720, USA

Roi Baer
Fritz Haber Center for Molecular Dynamics, Institute of Chemistry, The Hebrew University of Jerusalem, Jerusalem 91904, Israel

Daniel Neuhauser
Department of Chemistry and Biochemistry, University of California, Los Angeles, California 90095, USA

(Received 10 February 2015; revised manuscript received 25 April 2015; published 1 June 2015)

A time-dependent formulation for electron-hole excitations in extended finite systems, based on the Bethe-Salpeter equation (BSE), is developed using a stochastic wave function approach. The time-dependent formulation builds on the connection between time-dependent Hartree-Fock (TDHF) theory and the configuration-interaction with single substitution (CIS) method. This results in a time-dependent Schrödinger-like equation for the quasiparticle orbital dynamics based on an effective Hamiltonian containing direct Hartree and *screened* exchange terms, where screening is described within the random-phase approximation (RPA). To solve for the optical-absorption spectrum, we develop a stochastic formulation in which the quasiparticle orbitals are replaced by stochastic orbitals to evaluate the direct and exchange terms in the Hamiltonian as well as the RPA screening. This leads to an overall quadratic scaling, a significant improvement over the equivalent symplectic eigenvalue representation of the BSE. Application of the time-dependent stochastic BSE (TDsBSE) approach to silicon and CdSe nanocrystals up to size of ≈3000 electrons is presented and discussed.

DOI: 10.1103/PhysRevB.91.235302 PACS number(s): 71.10.−w, 71.15.Qe, 74.25.Jb

I. INTRODUCTION

Understanding electron-hole excitations in large molecular systems and nanostructures is essential for developing novel optical and electronic devices [1–4]. This is due, for example, to the exponential sensitivity of the photocurrent characteristics to the excitonic energy levels and the sensitivity of the device performance to the optical oscillator strength. It becomes, therefore, a necessity to develop accurate theoretical tools to describe the excitonic level alignment and the absorption spectrum, with computational complexity that is scalable to systems of experimental relevance (thousands of atoms and more).

There is no doubt that time-dependent density functional theory (TDDFT) [5] has revolutionized the field of electronic spectroscopy of small molecular entities [6–14]. TDDFT provides access to excited-state energies, geometries, and other properties of small molecules with a relatively moderate computational cost, similar to configuration interaction with single substitutions (CIS) in the linear-response frequency-domain formulation [15] [$O(N^4)$, where N is the number of electrons], or even better using a real-time implementation [16–18] [$O(N^2)$]. In principle TDDFT is exact but in practice approximations have to be introduced. The most common is the so-called time-dependent Kohn-Sham (TDKS) method within the adiabatic approximation, which has been applied to numerous challenging problems [19–43] with great success. However, TDKS often fails [44–52], particularly for charge-transfer excited states, multiple excitations, and avoided crossings. In the present context, perhaps the most significant failure of TDKS is in the description of low-lying excitonic states in bulk [53–57].

An alternative to TDDFT, which has mainly been applied to condensed periodic structures, is based on many-body perturbation theory (MBPT). The most common flavors are the GW approximation [58] to describe quasiparticle excitations (G indicates the single-particle Green function and W the screened Coulomb interaction) and the Bethe-Salpeter equation (BSE) [59] to describe electron-hole excitations. Both approaches offer a reliable solution to quasiparticle [60–78] and optical [53,54,56,57,66,79–89] excitations, even for situations where TDKS often fails, for example in periodic systems [53–57,79] or for charge-transfer excitations in molecules [86]. However, the computational cost of the MBPT methods is considerably more demanding than for TDKS, because conventional techniques require the explicit calculation of a large number of occupied and virtual electronic states and the evaluation of a large number of screened exchange integrals between valence and conduction states. This leads to a typical scaling of $O(N^6)$ and limits the practical applications of the BSE to small molecules or to periodic systems with small unit cells.

Significant progress has been made by combining ideas proposed in the context of TDDFT [90,91] and techniques used to represent the dielectric function [92] based on density functional perturbation theory [93]. This leads to an approach that explicitly requires only the occupied orbitals (and not the virtual states) and thus scales as $O(N^2 \times N_k^2 \times N_g)$ [57], where N_k is the number of points in the Brillouin zone and N_g is the size of the basis. Even with this more moderate scaling, performing a Bethe-Salpeter (BS) calculation for large systems with several thousands of electrons is still prohibitive.

Recently, we have proposed an alternative formulation for a class of electronic structure methods ranging from the density functional theory (DFT) [94,95], Møller-Plesset second-order perturbation theory (MP2) [96,97], the random-phase approximation (RPA) to the correlation energy [98], and even for multiexciton generation (MEG) [99]. But perhaps the most impressive formulations are that for calculating the quasiparticle energy within the *GW* many-body perturbation correction to DFT [100] and for a stochastic TDDFT [101]. The basic idea behind our formulation is that the occupied and virtual orbitals of the Kohn-Sham (KS) Hamiltonian are replaced by stochastic orbitals and the density and observables of interest are determined from an average of stochastic replicas in a trace formula. This facilitates "self-averaging" which leads to a report of sublinear scaling DFT electronic structure method (for the total energy per electron) and nearly linear scaling *GW* approach, breaking the theoretical scaling limit for *GW* as well as circumventing the need for energy cutoff approximations.

In this paper we develop an efficient approach for calculating electron-hole excitations (rather than charge excitations) based on the BSE, making it a practical and accessible computational tool for very large molecules and nanostructures. The BSE is often formulated in the frequency domain and thus requires the calculation of *screened* exchange integrals between occupied and virtual states. Instead, we introduce concepts based on stochastic orbitals and reformulate the BSE in the time domain as means of reducing CPU time and memory. The real-time formulation of the BSE delivers the response function (and thus the optical excitation spectrum) without requiring full resolution of the excitation energies, thereby reducing dramatically the computational cost. This is demonstrated for well-studied systems of silicon and CdSe nanocrystals, covering the size range $N \approx 100$–3000 electrons. Within this range, we show that the approach scales quadratically $[O(N^2)]$ with system size.

II. THEORY

In this section we review the symplectic eigenvalue formulation of the BSE and then build on the connections between configuration interaction with single substitution (CIS) and time-dependent Hartree-Fock (TDHF) to formulate a time-dependent wave equation for the BSE.

A. Symplectic eigenvalue Bethe-Salpeter equation

Within linear response, one can show that the BSE is equivalent to solving the symplectic eigenvalue problem [102–104]

$$\mathcal{L}\begin{pmatrix} X \\ Y \end{pmatrix} = \hbar\omega \begin{pmatrix} 1 & 0 \\ 0 & -1 \end{pmatrix}\begin{pmatrix} X \\ Y \end{pmatrix}, \tag{1}$$

where

$$\mathcal{L} = \begin{pmatrix} A & B \\ -B & -A \end{pmatrix} \tag{2}$$

with

$$\begin{aligned} A &= D + 2K^X + K^D, \\ B &= 2K^X + K^D. \end{aligned} \tag{3}$$

The diagonal (D), exchange (K^X), and direct (K^D) terms are given by (we use i, j, and $k\ldots$ as occupied (hole) state indices, a, b, and $c\ldots$ as unoccupied (electron) states indices, and r, s, and $t\ldots$ for general indices):

$$D_{ia,bj} = (\varepsilon_a - \varepsilon_i)\delta_{ab}\delta_{ij}, \tag{4}$$

$$K^X_{ia,bj} = \langle \phi_a\phi_i|\hat{v}_C|\phi_b\phi_j\rangle = \iint d\mathbf{r}d\mathbf{r}' \times \phi_i(\mathbf{r})\phi_a(\mathbf{r})v_C(|\mathbf{r}-\mathbf{r}'|)\phi_j(\mathbf{r}')\phi_b(\mathbf{r}'), \tag{5}$$

$$K^D_{ia,bj} = \langle \phi_a\phi_b|\hat{W}|\phi_i\phi_j\rangle = \iint d\mathbf{r}d\mathbf{r}'\phi_b(\mathbf{r})\phi_a(\mathbf{r})W(\mathbf{r},\mathbf{r}',0)\phi_j(\mathbf{r}')\phi_i(\mathbf{r}'). \tag{6}$$

Here, ε_a and ε_i are the quasiparticle energies for the virtual and occupied space (which can be obtained from a DFT + *GW* calculation or from an alternative suitable approach) and $\phi_a(\mathbf{r})$ and $\phi_i(\mathbf{r})$ are the corresponding quasiparticle orbitals; $\hat{v}_C$ is the Coulomb potential, while W is the screened Coulomb potential, typically calculated within the random-phase approximation (RPA), which can be written in real space as

$$W(\mathbf{r},\mathbf{r}',0) = v_C(|\mathbf{r}-\mathbf{r}'|) + \delta W^{\text{RPA}}(\mathbf{r},\mathbf{r}',0), \tag{7}$$

with

$$\delta W^{\text{RPA}}(\mathbf{r},\mathbf{r}',0) = \iint d\mathbf{r}''d\mathbf{r}'''v_C(|\mathbf{r}-\mathbf{r}''|)\tilde{\chi}^{\text{RPA}}(\mathbf{r}'',\mathbf{r}''',0) \times [v_C(|\mathbf{r}'''-\mathbf{r}'|) + f_{XC}(\mathbf{r}''')\delta(\mathbf{r}'''-\mathbf{r}')]. \tag{8}$$

Here, $f_{XC}(\mathbf{r})$ is the DFT exchange-correlation potential [if DFT is used to obtain the RPA screening, otherwise set $f_{XC}(\mathbf{r}) = 0$], and $\tilde{\chi}^{\text{RPA}}(\mathbf{r},\mathbf{r}',0)$ is the half-Fourier transform (at $\omega = 0$) of the real-time density-density correlation function within the RPA (the latter can be also obtained from TDDFT, as further discussed below). We note in passing that often the above is solved within the Tamm-Dancoff approximation (TDA) [105,106], which sets $B = 0$ and thus only requires the diagonalization of the matrix A.

B. Time-dependent Bethe-Salpeter equation (TDBSE)

The time-dependent formulation of the BSE follows from the connections made between CIS and TDHF [102,103,107,108]. In short, solving the TDHF equations $i\hbar\frac{\partial\phi_j(\mathbf{r},t)}{\partial t} = \hat{h}_{\text{HF}}(t)\phi_j(\mathbf{r},t)$ for the occupied orbitals is identical to solving the symplectic eigenvalue problem of Eq. (1) with $\delta W(\mathbf{r},\mathbf{r}',0) = 0$. Here, $\hat{h}_{\text{HF}} = \hat{t} + \hat{v}_{\text{ion}} + \hat{v}_H(t) + \hat{k}_X(t)$ is the Hartree-Fock (HF) Hamiltonian, $\hat{t}$ is the kinetic energy, $\hat{v}_{\text{ion}}$ is the external potential, $\hat{v}_H\psi(\mathbf{r}) = \int d\mathbf{r}'v_C(|\mathbf{r}-\mathbf{r}'|)n(\mathbf{r}',t)\psi(\mathbf{r})$ is the Hartree potential, and $\hat{k}_X(t)\psi(\mathbf{r}) = -\frac{1}{2}\int d\mathbf{r}'\rho(\mathbf{r},\mathbf{r}',t)v_C(|\mathbf{r}-\mathbf{r}'|)\psi(\mathbf{r}')$ is the nonlocal exchange potential. $n(\mathbf{r},t) = 2\sum_j |\phi_j(\mathbf{r},t)|^2$ and $\rho(\mathbf{r},\mathbf{r}',t) = 2\sum_j \phi_j^*(\mathbf{r}',t)\phi_j(\mathbf{r},t)$ are the time-dependent electron density and density matrix, respectively. The connection to CIS is made by realizing that for $\delta W(\mathbf{r},\mathbf{r}',0) = 0$ and setting $B = 0$ (the TDA), the symplectic eigenvalue problem of Eq. (1) is nothing else but the CIS Hamiltonian. Thus, TDHF within the TDA and CIS are identical.

We follow a similar logic and derive an adiabatic time-dependent BSE:

$$i\hbar\frac{\partial\phi_j^{\gamma}(\mathbf{r},t)}{\partial t}=\hat{h}_{\mathrm{BS}}^{\gamma}(t)\phi_j^{\gamma}(\mathbf{r},t),\tag{9}$$

where γ is a perturbation strength [i.e., $\gamma=0$ is the unperturbed case, see Eq. (12)] with a screened effective Hamiltonian given by

$$\hat{h}_{\mathrm{BS}}^{\gamma}=\hat{h}_{qp}+\hat{v}_H^{\gamma}(t)-\hat{v}_H^{0}(t)+\hat{k}_{\epsilon X}^{\gamma}(t)-\hat{k}_{\epsilon X}^{0}(t).\tag{10}$$

Before we discuss the different terms in Eq. (10), we note that the above Hamiltonian reduces to the HF limit for $\hat{k}_{\epsilon X}^{\gamma}(t)-\hat{k}_{\epsilon X}^{0}(t)=\hat{k}_{X}^{\gamma}(t)-\hat{k}_{X}^{0}(t)$ and $\hat{h}_{qp}=\hat{h}_{\mathrm{HF}}$, for the lowest order in γ. However, to describe a more general form of $\hat{h}_{qp}$ (for example the semiempirical model described below that is not self-consistent, one needs to subtract the unperturbed Hartree and exchange terms in $\hat{h}_{\mathrm{BS}}$. The subtraction is redundant for self-consistent models, such as the HF model of $\hat{h}_{qp}$.

In Eq. (10), $\hat{h}_{qp}$ is the quasiparticle Hamiltonian, namely, the Hamiltonian used to describe single-particle charge excitations. For example, such excitations can be determined from a *GW* calculation correcting the quasiparticle energies and orbitals of the underlying DFT. The *GW* approximation to $\hat{h}_{qp}$ is rather difficult to implement since it involves a nonlocal, energy-dependent operator. An alternative is to use a DFT approach that provides an accurate description of quasiparticle excitations., for example the nonlocal range separated functionals [109,110]. Since the exact model used for $\hat{h}_{qp}$ is not the central target of the present work, but rather how to obtain from it the optical (electron-hole) excitations, we represent it by a simple semiempirical local Hamiltonian of the form [111–117].

$$\hat{h}_{qp}\approx\hat{t}+\hat{v}_{ps},\tag{11}$$

where, as before, $\hat{t}$ is the kinetic energy and $\hat{v}_{ps}=\sum_{\alpha}\hat{v}_{\alpha}$ is the empirical pseudopotential, given as a sum of atomic pseudopotentials which were generated to reproduce the bulk band structure, providing accurate quasiparticle excitations in the bulk. The semiempirical approach has been successfully applied to calculate the quasiparticle spectrum of semiconducting nanocrystals of various sizes and shapes [111,113,116,118–122].

In Eq. (10), $\hat{v}_H^{\gamma}(t)\psi(\mathbf{r})=\int d\mathbf{r}'v_C(|\mathbf{r}-\mathbf{r}'|)n^{\gamma}(\mathbf{r}',t)\psi(\mathbf{r})$ is the Hartree potential with $n^{\gamma}(\mathbf{r},t)=2\sum_j|\phi_j^{\gamma}(\mathbf{r},t)|^2$ and $\hat{k}_{\epsilon X}^{\gamma}(t)\psi(\mathbf{r})=-\frac{1}{2}\int d\mathbf{r}'\rho^{\gamma}(\mathbf{r},\mathbf{r}',t)W^{\mathrm{RPA}}(\mathbf{r},\mathbf{r}',0)\psi(\mathbf{r}')$ is the screened exchange potential with $W^{\mathrm{RPA}}(\mathbf{r},\mathbf{r}',0)$ given by Eqs. (7) and (8) and $\rho^{\gamma}(\mathbf{r},\mathbf{r}',t)=2\sum_j\phi_j^{\gamma}(\mathbf{r}',t)^*\phi_j^{\gamma}(\mathbf{r},t)$. The application of $\hat{k}_{\epsilon X}^{\gamma}\psi(\mathbf{r})$ is further discussed below.

In analogy with the relations derived between TDHF and its eigenvalue representation, it is clear that the time-dependent formulation for the BSE given by Eqs. (9) and (10) is identical to the full symplectic eigenvalue problem of Eq. (1). In Fig. 1 we compare the results for $\mathrm{SiH_4}$ on an $8\times8\times8$ grid generated by propagating the occupied orbitals with the Bethe-Salpeter Hamiltonian (10) (TDBSE) to the exact diagonalization of Eq. (2) (static approach). We use a local semiempirical pseudopotential that has been applied successfully to study the optical properties of silicon nanocrystals [111,123,124]. For both the direct approach and the TDBSE we approximate $W(\mathbf{r},\mathbf{r}',0)$ by $\epsilon^{-1}v_C(|\mathbf{r}-\mathbf{r}'|)$, where ϵ is a constant screening parameter. The idea is to confirm that the eigenvalues of Eq. (2) and the time-dependent version of the BSE are identical (validating both the theory and the implementation).

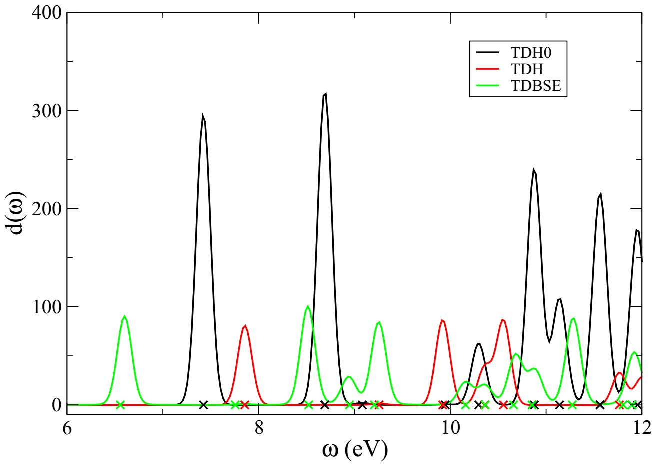

FIG. 1. (Color online) Comparison of BS calculations using the symplectic eigenvalue [Eq. (2), cross-symbol] with the frequency-dependent dipole-dipole correlation generated from TDBSE [Eqs. (9)–(11), solid lines] for $\mathrm{SiH_4}$. Black: TDBSE with $\gamma=0$ (TDH0) compared with eigenvalues of Eq. (2) setting K^X and K^D to zero. Red: TDBSE with $\hat{h}_{\mathrm{BS}}^{\gamma}=\hat{h}_{qp}+\hat{v}_H^{\gamma}(t)-\hat{v}_H^{0}(t)$ (TDH) compared with Eq. (2) setting K^D to zero (TDH). Green: TDBSE with $\gamma=10^{-5}$ a.u. (TDBSE) compared with Eq. (2), both for $\epsilon=5$.

The time-domain calculations are based on a linear-response approach to generate the dipole-dipole correlation function $d(t)$ and its Fourier transform $\tilde{d}(\omega)=\int_0^{\infty}dt\,e^{i\omega t}d(t)$. In short, we perturb the occupied eigenstates $[\phi_j(\mathbf{r})]$ of $\hat{h}_{qp}$ at $t=0$:

$$\phi_j^{\gamma}(\mathbf{r},t=0)=e^{-i\gamma z/\hbar}\phi_j(\mathbf{r}),\tag{12}$$

where, for simplicity, we assume that the dipole is in the z direction. We then propagate these orbitals according to Eq. (9) and generate the dipole-dipole correlation function:

$$d(t)=\frac{1}{\gamma}\int d\mathbf{r}\,z[n^{\gamma}(\mathbf{r},t)-n^{0}(\mathbf{r},t)],\tag{13}$$

where as before $n^{\gamma}(\mathbf{r},t)=2\sum_j|\phi_j^{\gamma}(\mathbf{r},t)|^2$and γ is a small parameter representing the strength of the perturbation, typically 10^{-3}–$10^{-5}\hbar E_h^{-1}$.

The agreement for the position of the excitations (solid lines) generated by the time-domain BSE is perfect with the static calculation (cross-symbol), as seen in Fig. 1. The resolved individual transitions are broadened reflecting the finite propagation time used for the time-domain calculations. We find that in some cases the oscillator strength is very small and thus a transition is not observed in $\tilde{d}(\omega)$.

An additional important test of the TDBSE formalism is whether the Hamiltonian in Eq. (10) preserves the Ehrenfest theorem (see Appendix B for more details). Naturally, this would be the case if $\hat{h}_{qp}$ would include the terms $\hat{v}_H^{0}(t)$ and $\hat{k}_{\epsilon X}^{0}(t)$, such that they cancel out for $\hat{h}_{\mathrm{BS}}^{\gamma}$. However, for an arbitrary choice of $\hat{h}_{qp}$ this needs to be confirmed. In Fig. 2 we plot the average momentum for $\mathrm{SiH_4}$ calculated in two

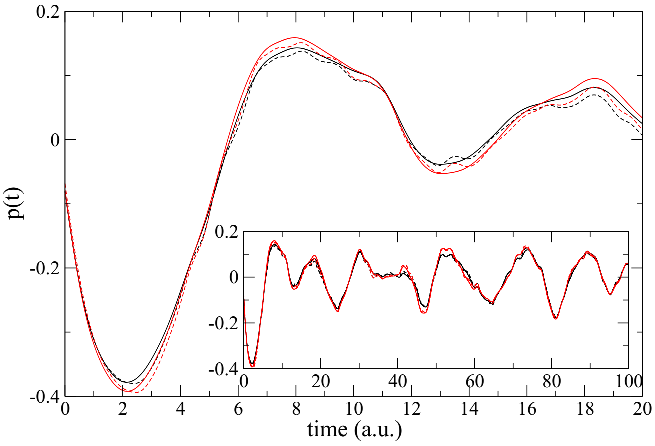

FIG. 2. (Color online) Average momentum along the z direction calculated in two ways (see text for more details) for SiH$_4$ using the TDH (black curves) and the TDBSE (red curves) methods. Solid and dashed curves where generated using the expectation value of the momentum [Eq. (14)] and the numerical derivative of the expectation value of the position [Eq. (15)], respectively. Inset: same for longer times.

different ways. The solid curves were obtained directly from

$$\frac{\langle \mathbf{p}(t)\rangle}{m} = -2i\hbar \sum_j \int d\mathbf{r}\phi_j^\gamma(\mathbf{r},t)^* \frac{\partial}{\partial \mathbf{r}} \phi_j^\gamma(\mathbf{r},t), \qquad (14)$$

while the dashed curves were obtained by taking the numerical time derivative (central difference) of the expectation value of $\mathbf{r}(t)$:

$$\frac{\langle \mathbf{p}(t)\rangle}{m} = \frac{\partial}{\partial t}\langle \mathbf{r}(t)\rangle = 2\frac{\partial}{\partial t} \sum_j \int d\mathbf{r}\phi_j^\gamma(\mathbf{r},t)^* \mathbf{r} \phi_j^\gamma(\mathbf{r},t). \qquad (15)$$

The agreement is not perfect but improves with decreasing the time step δt (not shown here). We also show the results for the time-dependent Hartree (TDH), i.e., ignoring the screened exchange term in $\hat{h}_{\mathrm{BS}}^\gamma$. The deviations observed for TDBSE and TDH are similar, although for TDH the Ehrenfest theorem holds exactly and thus the agreement should be perfect. The difference are associated with numerical inaccuracies resulting from the finite time step and grid used in the calculation. The inset shows that the deviations are insignificant even at much longer times over many periods.

III. TIME-DEPENDENT STOCHASTIC BETHE-SALPETER EQUATION

We consider two formulations for the time-dependent stochastic BSE (TDsBSE). The first approach is a direct generalization of the approach we have recently developed for the stochastic TDH [101], in which we describe an efficient way to account for the screened exchange term in the $\hat{h}_{\mathrm{BS}}^\gamma$. This approach works well for short times, however, unlike in TDH, the inclusion of an exchange term requires an increasing number of stochastic orbitals with the system size. The second approach offers access to time scales relevant for most spectroscopic applications at a practical quadratic computational cost.

A. Extending the stochastic TDH to include a screened exchange term

We limit the discussion, in the body of this paper, to the case where $W(\mathbf{r},\mathbf{r}',0)$ is replaced by $\epsilon^{-1} v_C(|\mathbf{r}-\mathbf{r}'|)$, where ϵ is a function of $|\mathbf{r}-\mathbf{r}'|$. The algorithm for the TDsBSE is based on the following steps:

(1) Generate N_ζ stochastic orbitals $\zeta_j(\mathbf{r}) = e^{i\theta_j(\mathbf{r})}/\sqrt{\delta V}$, where $\theta_j(\mathbf{r})$ is a uniform random variable in the range $[0,2\pi]$ at each grid point (total of N_g grid points), δV is the volume element of the grid, and $j = 1,\ldots,N_\zeta$. The stochastic orbitals obey the relation $\mathbf{1} = \langle |\zeta\rangle\langle\zeta|\rangle_\zeta$ where $\langle\cdots\rangle_\zeta$ denotes a statistical average over ζ.

(2) Project each stochastic orbital $\zeta_j(\mathbf{r})$ onto the occupied space: $|\xi_j\rangle \equiv \sqrt{\theta_\beta(\mu - \hat{h}_{qp})}|\zeta_j\rangle$, where $\theta_\beta(x) = \frac{1}{2}\mathrm{erfc}(\beta(x))$ is a smooth representation of the Heaviside step function [94] and μ is the chemical potential. The action of $\sqrt{\theta_\beta}$ is performed using a suitable expansion in terms of Chebyshev polynomials in the static quasiparticle Hamiltonian with coefficients that depend on μ and β [125].

(3) Define nonperturbed and perturbed orbitals at $t = 0$: $\xi_j^0(\mathbf{r},t=0) = \xi_j(\mathbf{r})$, $\xi_j^\gamma(\mathbf{r},t=0) = e^{-iv(\mathbf{r})/\hbar}\xi_j(\mathbf{r})$. For the absorption spectrum, the perturbation is given by $v(\mathbf{r}) = r_\alpha$ and $\alpha \equiv x,y,z$.

(4) Propagate the perturbed $[\xi_j^\gamma(\mathbf{r},t)]$ and unperturbed $[\xi_j^0(\mathbf{r},t)]$ orbitals according to the adiabatic time-dependent BSE:

$$i\hbar\frac{\partial \xi_j^\gamma(\mathbf{r},t)}{\partial t} = \hat{h}_{\mathrm{BS}}^\gamma(t)\xi_j^\gamma(\mathbf{r},t). \qquad (16)$$

Use the split operator technique to perform the time propagation from time t to time $t+\Delta t$:

$$\begin{aligned} e^{-(i/\hbar)\hat{h}_{\mathrm{BS}}^\gamma \Delta t} \approx{}& e^{-(i/2\hbar)(\hat{v}_{ps}+\hat{v}_H^\gamma(t)-\hat{v}_H^0(t))\Delta t} \\ &\times e^{-(i/2\hbar)\hat{t}\Delta t} e^{-(i/\hbar)(\hat{k}_{\epsilon X}^\gamma(t)-\hat{k}_{\epsilon X}^0(t))\Delta t} \\ &\times e^{-(i/2\hbar)\hat{t}\Delta t} e^{-(i/2\hbar)(\hat{v}_{ps}+\hat{v}_H^\gamma(t)-\hat{v}_H^0(t))\Delta t}, \end{aligned} \qquad (17)$$

where the propagator step involving the nonlocal screened exchange is applied using a Taylor series (in all applications below we used a first order Taylor expansion)

$$e^{-(i/\hbar)(\hat{k}_{\epsilon X}^\gamma(t)-\hat{k}_{\epsilon X}^0(t))\Delta t} \approx 1 - \frac{i}{\hbar}\left(\hat{k}_{\epsilon X}^\gamma(t) - \hat{k}_{\epsilon X}^0(t)\right)\Delta t + \cdots . \qquad (18)$$

(5) The application of $\hat{h}_{\mathrm{BS}}^\gamma(t)$ is done as follows:

(a) The kinetic energy is applied using a fast Fourier transform (FFT).

(b) The Hartree term is generated using convolution and FFT with the density obtained from the stochastic orbitals:

$$n^\gamma(\mathbf{r},t) = \frac{2}{N_\zeta}\sum_{j=1}^{N_\zeta} \left|\xi_j^\gamma(\mathbf{r},t)\right|^2. \qquad (19)$$

(c) The time-consuming part of the application of $\hat{h}_{\mathrm{BS}}^\gamma$ on a vector ψ in Hilbert space is $\hat{k}_{\epsilon X}^\gamma(t) - \hat{k}_{\epsilon X}^0(t)$. This operation scales as $O(NN_g)$ and one needs to carry this for all occupied states, leading a $O(N^2N_g)$ computational scaling. To reduce this high scaling resulting from the exchange operation we use the same philosophy underlying this work, i.e., replacing summation with stochastic averaging. In practice we therefore

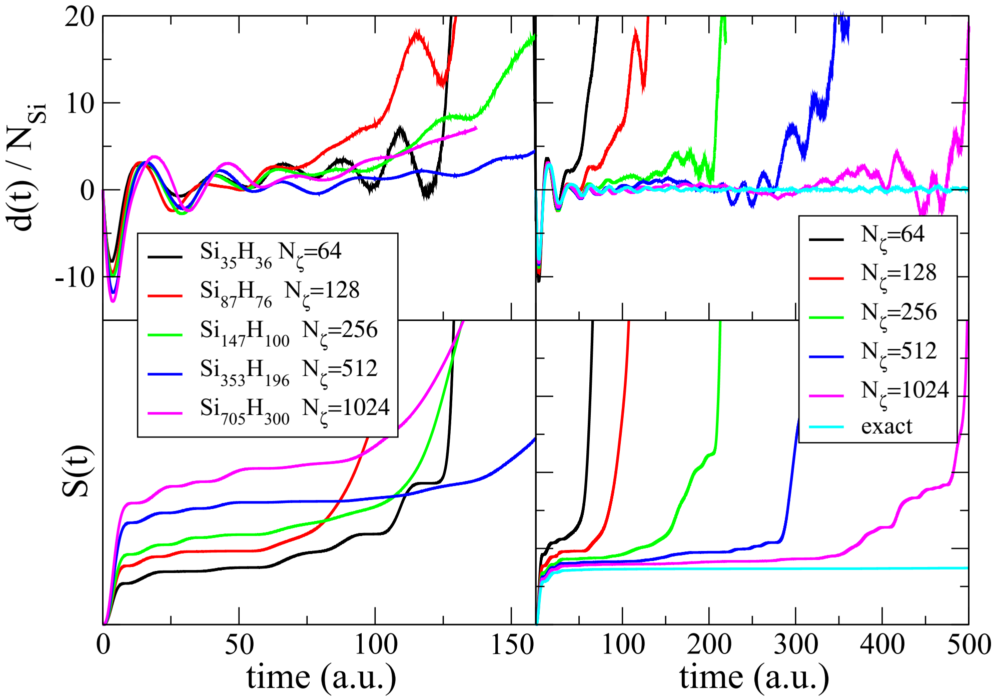

FIG. 3. (Color online) Upper left: Dipole-dipole correlation function [Eq. (13)] normalized to the number of silicon atoms in the nanocrystal (N_{Si}) for several nanocrystal sizes. For each size we use a different number of stochastic orbitals. Lower left: Integrate dipole-dipole correlation $S(t) = \int_0^t ds\, d(s)^2$. The onset of divergence scales roughly linearly with the size. Upper right: Dipole-dipole correlation function normalized to the number of silicon atoms for $Si_{87}H_{76}$ for different values of N_ζ. Lower right: Corresponding values for $S(t)$.

replace the summation over occupied orbitals in the exchange operation by acting with very few $n_\eta \ll N_\zeta$, typically $n_\eta = 1$–16, stochastic orbitals and write the exchange operation as

$$\hat{k}^{\gamma}_{\epsilon X}(t)\psi(\mathbf{r},t) = \frac{1}{n_\eta}\sum_{x=1}^{n_\eta} \eta_x^{\gamma}(\mathbf{r},t)\int d\mathbf{r}'\epsilon^{-1} v_C(|\mathbf{r}-\mathbf{r}'|)\eta_x^{\gamma}(\mathbf{r}',t)^{*}\psi(\mathbf{r}',t). \tag{20}$$

The key is that these stochastic orbitals are defined as a different random combination of the full set of orbitals at any given time step; η_x^γ are defined as random superpositions of the N_ζ stochastic orbitals:

$$\eta_x^{\gamma}(\mathbf{r},t) = \frac{1}{N_\zeta}\sum_{j}^{N_\zeta} e^{i\alpha_{xj}(t)}\xi_j^{\gamma}(\mathbf{r},t). \tag{21}$$

To improve the representation of the stochastic exchange operators, the random phases $\alpha_{xj}(t)$ are resampled at each time step. Note that the same phases are used for both $\eta_x^\gamma(\mathbf{r},t)$ and $\eta_x^0(\mathbf{r},t)$. This use of stochastic orbitals reduces the overall scaling of the method to quadratic, since n_η does not depend on the system size.

In Fig. 3 we show the calculated $d(t)$ and $S(t) = \int_0^t ds\, d(s)^2$ for a series of silicon nanocrystals. We used $n_\zeta = 16$ which leads to results that are indistinguishable from $n_\zeta = N_\zeta$ (though even a smaller n_ζ would have been sufficient). We used a constant value for $\epsilon = 5$ and the time step was $\Delta t = 0.025$ a.u.

In general, we find that the results converge up to a time τ_C and then the signal diverges exponentially. Several conclusions can be drawn from these calculations, as follows:

(1) The stochastic approximation to $d(t)$ oscillates about zero up to a time τ_C, but this is followed by a gradual increase which eventually leads to divergence (upper panels of Fig. 3).

(2) τ_C increases with the number of stochastic orbitals, N_ζ, roughly as $\tau_C \propto N_\zeta^\alpha$ with $\alpha = 1$–2 (right panels of Fig. 3). This is somewhat better than the case for TDH for which τ_C roughly scaled as $N_\zeta^{1/2}$.

(3) τ_C decreases with increasing system size roughly as $\frac{1}{N}$, where N is the number of electrons (left panels of Fig. 3). Therefore, to converge the results to a fixed τ_C one has to increase N_ζ roughly linearly with the system size. This leads to a quadratic scaling of the approach. In TDH the opposite is true, τ_C *increases* with increasing system size due to self-averaging [101].

(4) To reach times sufficient for most spectroscopic applications, the number of stochastic orbitals exceeds that of occupied states ($N_\zeta > N_{\text{occ}}$).

To conclude this subsection, we find that this version of a TDsBSE scales roughly quadratically with the system size, rather than sublinearly for TDH. Furthermore, to calculate the response to meaningful times, the naive extension of the TDH to include exchange requires a rather large number of stochastic orbitals (N_ζ), often much larger than the number of occupied orbitals. However, it is sufficient to represent the operation of the exchange Hamiltonian with a relatively small set of linear combination of all stochastic orbitals (n_ζ). We next show how the method can be improved significantly increasing τ_C to values much larger than required to obtain the spectrum in large systems.

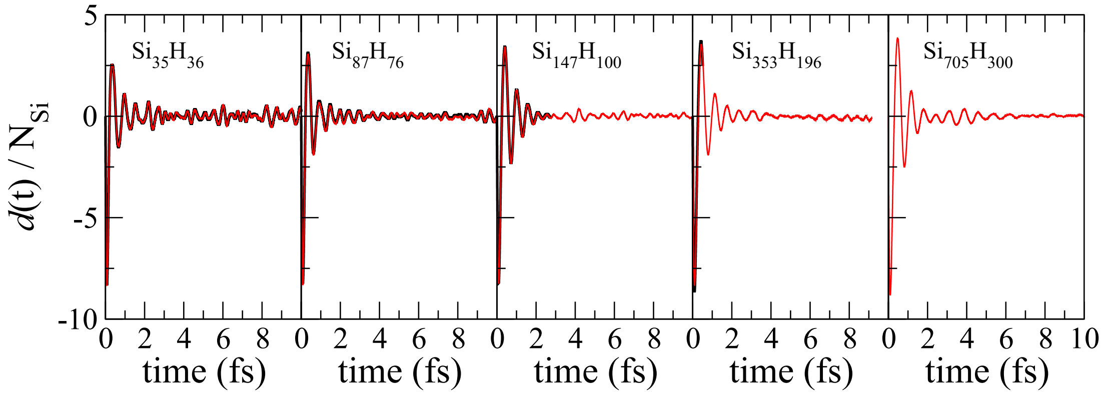

FIG. 4. (Color online) The dipole-dipole correlation function calculated using the TDsBSE approach with orthogonalization (red curves) compared with a direct time-dependent BSE approach (black curves). Note that the direct (i.e., nonstochastic) BSE approach is so expensive due to the full-exchange operation that it was not done for the largest NCs and was only followed for short times for intermediate size NCs.

B. Time-dependent stochastic Bethe-Salpeter with orthogonalization

To circumvent the pathological behavior observed above, we propose to orthogonalize the projected stochastic orbitals (after step "2"). This requires that N_ζ be equal to the number of occupied states $N_{\rm occ}$. However, this makes the TDsBSE stable for time scales exceeding 50 fs, which for any practical spectroscopic application for large systems is more than sufficient. Formally, since the number of stochastic orbitals (equal to the number of occupied states) increases linearly with the system size, the approach scales as $O(N_\zeta N_g)$. The orthogonalization step scales formally as $O(N_\zeta^2 N_g)$, however, for the size of systems studied here, it is computationally negligible compared with the projection and propagation steps.

In Fig. 4 we compare the dipole-dipole correlation function computed from the TDsBSE with $n_\zeta = 1$ to the direct TDBSE approach for silicon nanocrystals (NCs) of varying sizes ($Si_{35}H_{36}$, $Si_{87}H_{76}$, $Si_{147}H_{100}$, $Si_{353}H_{196}$, and $Si_{705}H_{300}$). The purpose is to demonstrate the power of the TDsBSE approach with orthogonalization. Therefore, for simplicity $W(\mathbf{r},\mathbf{r}',0)$ is replaced by $\epsilon^{-1} v_C(|\mathbf{r}-\mathbf{r}'|)$ with $\epsilon = 5$ for all system sizes. Clearly, even when $n_\zeta = 1$, the TDsBSE is in perfect

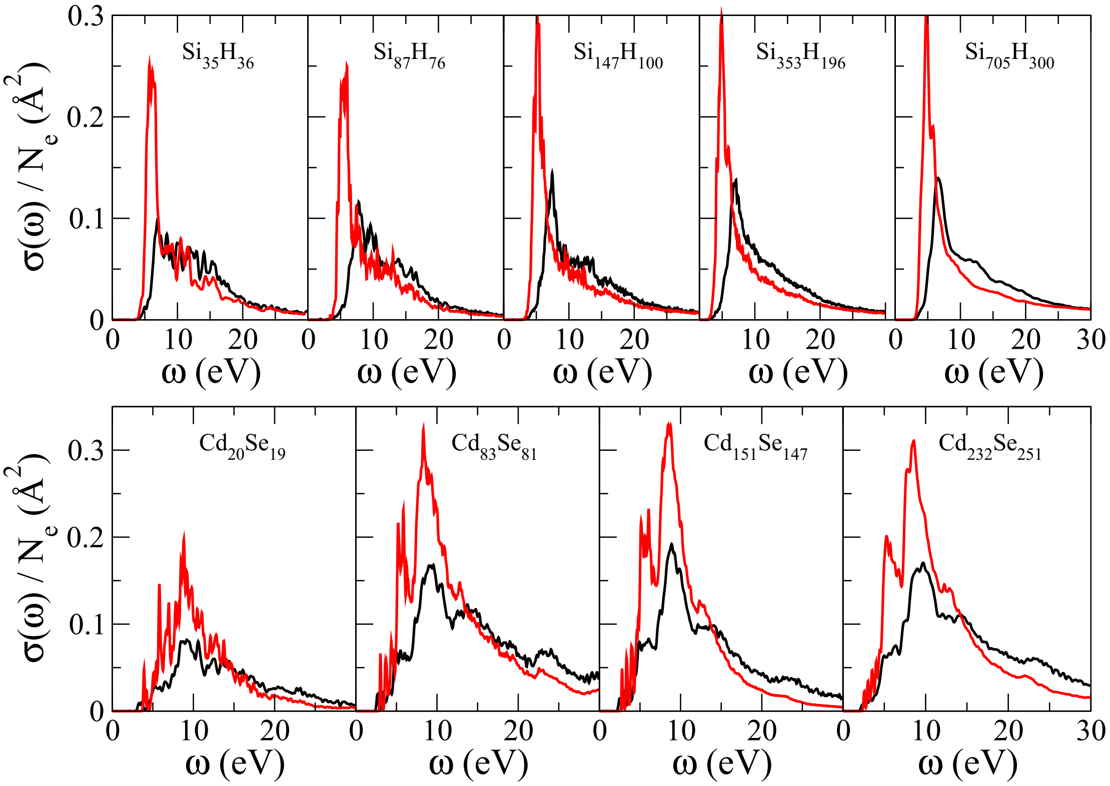

FIG. 5. (Color online) Upper panels: The absorption cross section for silicon NCs computed by Fourier transforming the TDsBSE dipole-dipole correlation function (black curves) and the corresponding absorption cross section computed for $\hat{h}_{qp}$, i.e., by ignoring electron-hole interactions.

agreement with the direct TDBSE approach. The cubic scaling of the latter limits the application to small NCs or to short times.

In Fig. 5 we plot the TDsBSE absorption cross section ($\sigma(\omega) = \frac{e^2}{\epsilon_0 c}\omega \int dt e^{i\omega t} \frac{1}{\gamma} \int d\mathbf{r}\, z[n^{\gamma}(\mathbf{r},t) - n^{0}(\mathbf{r},t)]$) compared to the absorption cross section computed by ignoring the electron-hole interactions for a wide range of energies. It is practically impossible to obtain the absorption cross section over this wide energy range by a direct diagonalization of the symplectic eigenvalue equation [cf. Eq. (1)]. Thus, so far the BSE has been applied to relatively small nanocrystals or by converging only the low-lying excitonic transitions, even within the crude approximation where $W(\mathbf{r},\mathbf{r}',0)$ is replaced by $\epsilon^{-1} v_C(|\mathbf{r} - \mathbf{r}'|)$. The results shown in Fig. 5 report a converged BS calculation for NCs of experimentally relevant sizes. We used a constant ϵ in each run, with values of 5, 6.2, 7, 8.2, and 8.8 taken from Ref. [123] for the silicon NCs (in ascending order) and 4.5, 5, 5.2 and 5.4 for the CdSe NCs taken from Ref. [113]. The inclusion of a more accurate description of the screening as proposed in detail in Appendix A is left open for future study.

For both types of NCs there is a shift of the onset of absorption to lower energies with increasing NC size due to the quantum confinement effect. The absorption cross section of the smallest NCs is characterized by detailed features, which are broadened and eventually washed out as the NC size increases. For silicon NCs, the semiempirical pseudopotential model overemphasizes the lowest excitonic transition in comparison to the plasmonic resonance observed at ∼10 eV using TDDFT [35,56,66,101]. It also misses the split of the lowest excitonic peak observed experimentally for bulk silicon and reproduced by the BSE approach [54–57], but not by the current model ignoring electron-hole correlations [123]. The fact that the current calculation does not capture this split could be a consequence of the approximation used to model the screening.

The results for silicon NCs seem to imply that the inclusion of electron-hole interactions leads to a blueshift in the absorption cross section (the black curve is shifted to higher energies compared to the red curve). Since silicon is an indirect band-gap material, the onset of absorption is not a good measure of the strength of the electron-hole interactions. Indeed, when the approach is applied to CdSe NCs (lower panels of Fig. 5) the inclusion of electron-hole interaction clearly shifts the onset of absorption to lower energies.

IV. CONCLUSIONS

We have developed a real-time stochastic approach to describe electron-hole excitations in extended finite systems based on the BSE. Following the logic connecting TDHF and CIS, we showed that a solution to a Schrodinger-like time-dependent equation for the quasiparticle orbitals with an effective Hamiltonian containing both direct and screened exchange terms is equivalent to the symplectic eigenvalue representation of the BSE. A direct solution of the TDBSE leads to at least cubic scaling with the system size due to the need to compute all occupied quasiparticle orbitals and the complexity of applying the screened exchange term to preform the time propagation. The lower bound is similar to the scaling of the TDHF method and thus, limits the application of the TDBSE approach to relatively small systems. To overcome this bottleneck, we developed a stochastic approach inspired by our previous work on stochastic *GW* [100] (s*GW*) and stochastic TDDFT [101] in which the occupied quasiparticle orbitals were replaced with stochastic orbitals. The latter can be used to obtain both the RPA screening using the approach developed for the screening in s*GW* and the exchange potential by extending the approach used to describe the Hartree term in TDsDFT. However, to provide a proof of principle of the TDsBSE approach, we have used a simplified screening procedure for the exchange term, replacing the dielectric tensor by a static dielectric constant.

Both the RPA screening and the application of the exchange potential scale nearly linearly with system size (as opposed to quadratic scaling for example for the exchange potential). The number of stochastic orbitals required to converge the calculation also scales linearly with system size and thus the overall scaling of the TDsBSE approach is quadratic (excluding the cubic contribution from the orthogonalization of the stochastic orbitals, which for the system sizes studied here is a negligible step). The improved overall scaling implies that the current approach will eventually outperform standard techniques as the system size increases (we believe that this is already the case for the largest system studied in this work). However, the crossover in performance between the stochastic and frequency domain implementations will depend on several factors, including the specific system and implementation as well as how well the algorithm can be parallelized.

We have applied the TDsBSE approach to study optical excitations in a wide range of energies (up to 30 eV) in silicon and CdSe nanocrystals with sizes up to ≈3000 electrons (≈3 nm diameter) and compared the results with the quasiparticle excitation spectrum obtained within the semiempirical pseudopotential approach. For both systems, we find that including electron-hole correlations broadens the spectral features and shifts the oscillator strength to higher energies due to amplification of a plasmon resonance near 10 eV. For silicon we find a surprising result where the onset optical excitations seem to shift to higher energies compared to the quasiparticle excitations. This is a result of two factors. First, silicon is an indirect band-gap material and the onset of optically allowed transitions is above the lowest excitonic state. Second, the inclusion of electron-hole interactions via the BSE leads to an amplification of a plasmon resonance at ≈10 eV shifting the oscillator strength to higher energies at the expense of the lower frequency absorption. These combined effects lead to an apparent shift of the absorption onset to higher energies when electron-hole interactions are included. This is not the case for CdSe, where the onset of optical excitation is below the onset of the quasiparticle excitation, as expected for a direct band-gap material.

The TDsBSE provides a platform to obtain optical excitations in extended systems covering a wide energy range. To overcome the divergent behavior at long times, it is necessary to increase the number of stochastic orbitals as the size of the system increases. We are working on improvements to this flaw and if solved, an even faster, linear scaling BS approach will emerge. This and other improvements as well as more general applications will be presented in a future work.

ACKNOWLEDGMENTS

We thank the Israel Science Foundation–FIRST Program (Grant No. 1700/14). D.N. acknowledges support by the National Science Foundation (NSF), Grant No. CHE-1112500.

APPENDIX A: RPA SCREENED EXCHANGE FOR TDsBSE

The above approach assumes that $W(\mathbf{r},\mathbf{r}',0) = v_C(|\mathbf{r}-\mathbf{r}'|) + \delta W_{\text{RPA}}(\mathbf{r},\mathbf{r}',0)$ is approximated by $\epsilon^{-1} v_C(|\mathbf{r}-\mathbf{r}'|)$. In typical BS applications, one uses the RPA screening to describe $W(\mathbf{r},\mathbf{r}',0) = v_C(|\mathbf{r}-\mathbf{r}'|) + \delta W(\mathbf{r},\mathbf{r}',0)$. The stochastic formalism, however, furnishes a potentially viable approach to overcome the assumption made to obtain $W(\mathbf{r},\mathbf{r}',0)$ in this work. In the linear-response limit, $\delta W_{\text{RPA}}(\mathbf{r},\mathbf{r}',0)$ can be written as

$$\delta W_{\text{RPA}}(\mathbf{r},\mathbf{r}',0) = \iint d\mathbf{r}'' d\mathbf{r}''' v_C(|\mathbf{r}-\mathbf{r}''|)\tilde{\chi}_{\text{RPA}}(\mathbf{r}'',\mathbf{r}''',0) \times [v_C(|\mathbf{r}'''-\mathbf{r}'|) + f_{XC}(\mathbf{r}''')\delta(\mathbf{r}'''-\mathbf{r}')], \tag{A1}$$

and we are concerned with the application of $\hat{k}^{\gamma}_{\epsilon X}(t)$ on $\psi(\mathbf{r},t)$, or more accurately, the portion that depends on the screening:

$$\delta\hat{k}^{\gamma}_{\epsilon X}(t) = \eta^{\gamma}_{x}(\mathbf{r},t) \int d\mathbf{r}' \delta W_{\text{RPA}}(\mathbf{r},\mathbf{r}',0) \eta^{\gamma}_{x}(\mathbf{r}',t)^{*} \psi(\mathbf{r}',t). \tag{A2}$$

We first insert Eq. (8) into Eq. (A2):

$$\begin{aligned}\delta\hat{k}^{\gamma}_{\epsilon X}(t)\psi(\mathbf{r},t) &= \eta^{\gamma}_{x}(\mathbf{r},t) \iint \int d\mathbf{r}' d\mathbf{r}'' d\mathbf{r}''' \\ &\times v_C(|\mathbf{r}-\mathbf{r}''|)\tilde{\chi}_{\text{RPA}}(\mathbf{r}'',\mathbf{r}''',0)[v_C(|\mathbf{r}'''-\mathbf{r}'|) \\ &+ f_{XC}(\mathbf{r}''')\delta(\mathbf{r}'''-\mathbf{r}')]\eta^{\gamma}_{x}(\mathbf{r}',t)^{*}\psi(\mathbf{r}',t).\end{aligned} \tag{A3}$$

Define a perturbation potential

$$v^{\gamma}(\mathbf{r},t) = \int d\mathbf{r}'[v_C(|\mathbf{r}'''-\mathbf{r}'|) + f_{XC}(\mathbf{r}''')\delta(\mathbf{r}'''-\mathbf{r}')] \times \eta^{\gamma}_{x}(\mathbf{r}',t)^{*}\psi(\mathbf{r}',t) \tag{A4}$$

and rewrite Eq. (A3) as

$$\delta\hat{k}^{\gamma}_{\epsilon X}(t)\psi(\mathbf{r},t) = \eta^{\gamma}_{x}(\mathbf{r},t) \iint d\mathbf{r}' d\mathbf{r}'' v_C(|\mathbf{r}-\mathbf{r}'|) \times \tilde{\chi}_{\text{RPA}}(\mathbf{r}',\mathbf{r}'',0) v^{\gamma}(\mathbf{r}'',t). \tag{A5}$$

The action of $\tilde{\chi}_{\text{RPA}}(\mathbf{r}',\mathbf{r}'',0)$ on $v^{\gamma}(\mathbf{r}'',t)$ is manageable by using a stochastic TDDFT algorithm [101]:

(1) Take N_{RPA} projected stochastic orbitals from the N_{ζ} generated above. If $N_{\text{RPA}} > N_{\zeta}$, generate additional projected stochastic orbitals following the prescription given in steps 1 and 2 above. This needs to be done just once, i.e., at the beginning of the calculation, generate enough projected stochastic orbitals to be used throughout the calculation.

(2) Apply a perturbation at $\tau = 0$: $\chi^{\gamma'}_{j}(\mathbf{r},\tau=0) = e^{-i\gamma' v^{\gamma}(\mathbf{r},t)/\hbar}\xi_j(\mathbf{r})$, where γ' is the strength of the RPA perturbation. Note that at each time t used for solving the TDsBSE, one has to apply a different perturbation $v^{\gamma}(\mathbf{r},t)$ at $\tau = 0$, which is used to indicate the time for the RPA propagation.

(3) Propagate the orbitals using the adiabatic stochastic time-dependent equations:

$$i\hbar \frac{\partial \chi^{\gamma'}_{j}(\mathbf{r},\tau)}{\partial \tau} = \hat{h}^{\gamma'}_{\text{RPA}}(\tau)\chi^{\gamma'}_{j}(\mathbf{r},\tau). \tag{A6}$$

Here, one can take $\hat{h}^{\gamma'}_{\text{RPA}}(\tau) = \hat{h}_{qp}$ or $\hat{h}^{\gamma'}_{\text{RPA}}(\tau) = \hat{h}_{qp} + v_{\text{HXC}}[n^{\gamma'}_{\text{RPA}}(\tau)](\mathbf{r}) - v_{\text{HXC}}[n^{0}_{\text{RPA}}(\tau)](\mathbf{r})$. For the latter case, $v_{\text{HXC}}[n](\mathbf{r}) = \int d\mathbf{r}' \frac{n(\mathbf{r}')}{|\mathbf{r}-\mathbf{r}'|} + v_{XC}(n(\mathbf{r}))$ and $v_{XC}(n(\mathbf{r}))$ is the local density (or semilocal) approximation for the exchange correlation potential. The density is obtained as an *average* over the RPA stochastic orbital densities:

$$n^{\gamma'}_{\text{RPA}}(\mathbf{r},\tau) = \frac{2}{N_{\text{RPA}}} \sum_{j=1}^{N_{\text{RPA}}} \left|\chi^{\gamma'}_{j}(\mathbf{r},\tau)\right|^2. \tag{A7}$$

(4) Generate $\Delta n_{\text{RPA}}(\mathbf{r},\tau) = \frac{1}{\gamma'}(n^{\gamma'}_{\text{RPA}}(\mathbf{r},\tau) - n^{0}_{\text{RPA}}(\mathbf{r},\tau))$ and its half Fourier transformed quantity $\Delta\tilde{n}_{\text{RPA}}(\mathbf{r},0)$ at $\omega = 0$.

(5) Obtain the action of $\delta\hat{k}^{\gamma}_{\epsilon X}(t)\psi(\mathbf{r},t) = \eta^{\gamma}_{x}(\mathbf{r},t) \iint d\mathbf{r}' d\mathbf{r}'' v_C(|\mathbf{r}-\mathbf{r}'|)\tilde{\chi}_{\text{RPA}}(\mathbf{r}',\mathbf{r}'',0)v^{\gamma}(\mathbf{r}'',t)$ from $\delta\hat{k}_{\epsilon X}(t) \psi(\mathbf{r},t) = \eta^{\gamma}_{x}(\mathbf{r},t) \iint d\mathbf{r}' d\mathbf{r}'' v_C(|\mathbf{r}-\mathbf{r}'|)\Delta\tilde{n}_{\text{RPA}}(\mathbf{r}',0)$.

Steps 1–5 need to be repeated at each time step Δt of the TDsBSE propagation.

APPENDIX B: EHRENFEST THEOREM

Ehrenfest theorem asserts that a correct propagation must preserve the relation

$$\langle \dot{\mathbf{r}}(t) \rangle = i\left\langle \left[\hat{h}_{\text{BS}},\hat{\mathbf{r}}\right]\right\rangle. \tag{B1}$$

For a TDBSE this relation is given by

$$i\langle[\hat{h}_{\text{BS}},\hat{\mathbf{r}}]\rangle = \frac{\langle \mathbf{p}(t) \rangle}{m} + i\left\langle\left[\hat{k}^{\gamma}_{\epsilon X}(t) - \hat{k}^{0}_{\epsilon X}(t),\hat{\mathbf{r}}\right]\right\rangle, \tag{B2}$$

where $\hat{k}^{\gamma}_{\epsilon X}(t)\psi(\mathbf{r}) = -\frac{1}{2}\int d\mathbf{r}' \rho^{\gamma}(\mathbf{r},\mathbf{r}',t) W^{\text{RPA}}(\mathbf{r},\mathbf{r}',0)\psi(\mathbf{r}')$. To satisfy the Ehrenfest theorem $\langle[\hat{k}^{\gamma}_{\epsilon X}(t) - \hat{k}^{0}_{\epsilon X}(t),\hat{\mathbf{r}}]\rangle$ should vanish. The commutator of the exchange operator is given by

$$i\left\langle\left[\hat{k}^{\gamma}_{\epsilon X}(t),\hat{\mathbf{r}}\right]\right\rangle = -\frac{i}{2}\iint d^3r d^3r' |\rho^{\gamma}(\mathbf{r},\mathbf{r}',t)|^2 \times W^{\text{RPA}}(\mathbf{r},\mathbf{r}',0)(\mathbf{r}-\mathbf{r}'). \tag{B3}$$

In the above, the commuter vanishes for the $\hat{k}^{\gamma}_{\epsilon X}(t)$ term due to symmetry, but there is no *a priori* reason why the $\hat{k}^{0}_{\epsilon X}(t)$ term should vanish. However, as illustrated numerically in Fig. 2, the contribution of this nonvanishing term is rather small even on time scales much larger than the typical frequency in the system.

[1] S. Coe, W.-K. Woo, and V. B. Moungi Bawendi, Nature (London) **420**, 800 (2002).

[2] N. Tessler, V. Medvedev, M. Kazes, S. H. Kan, and U. Banin, Science **295**, 1506 (2002).

[3] I. Gur, N. A. Fromer, M. L. Geier, and A. P. Alivisatos, Science **310**, 462 (2005).

[4] D. V. Talapin and C. B. Murray, Science **310**, 86 (2005).

[5] E. Runge and E. K. U. Gross, Phys. Rev. Lett. **52**, 997 (1984).

[6] R. van Leeuwen, Int. J. Mod. Phys. B **15**, 1969 (2001).

[7] G. Onida, L. Reining, and A. Rubio, Rev. Mod. Phys. **74**, 601 (2002).

[8] N. T. Maitra, K. Burke, H. Appel, and E. K. U. Gross, in *Reviews in Modern Quantum Chemistry: A Celebration of the Contributions of R. G. Parr*, edited by K. D. Sen (World Scientific, Singapore, 2002), Vol. II, p. 1186.

[9] M. Marques and E. Gross, Annu. Rev. Phys. Chem. **55**, 427 (2004).

[10] K. Burke, J. Werschnik, and E. K. U. Gross, J. Chem. Phys. **123**, 062206 (2005).

[11] S. Botti, A. Schindlmayr, R. Del Sole, and L. Reining, Rep. Prog. Phys. **70**, 357 (2007).

[12] D. Jacquemin, E. A. Perpete, I. Ciofini, and C. Adamo, Acc. Chem. Res. **42**, 326 (2009).

[13] M. E. Casida, J. Mol. Struct. **914**, 3 (2009).

[14] C. Adamo and D. Jacquemin, Chem. Soc. Rev. **42**, 845 (2013).

[15] R. E. Stratmann, G. E. Scuseria, and M. J. Frisch, J. Chem. Phys. **109**, 8218 (1998).

[16] K. Yabana and G. F. Bertsch, Phys. Rev. B **54**, 4484 (1996).

[17] G. F. Bertsch, J. I. Iwata, A. Rubio, and K. Yabana, Phys. Rev. B **62**, 7998 (2000).

[18] R. Baer and D. Neuhauser, J. Chem. Phys. **121**, 9803 (2004).

[19] R. Bauernschmitt and R. Ahlrichs, Chem. Phys. Lett. **256**, 454 (1996).

[20] R. Bauernschmitt, R. Ahlrichs, F. H. Hennrich, and M. M. Kappes, J. Am. Chem. Soc. **120**, 5052 (1998).

[21] J. Fabian, Theor. Chem. Acc. **106**, 199 (2001).

[22] I. Vasiliev, S. Ogut, and J. R. Chelikowsky, Phys. Rev. B **65**, 115416 (2002).

[23] Y. H. Shao, M. Head-Gordon, and A. I. Krylov, J. Chem. Phys. **118**, 4807 (2003).

[24] M. C. Troparevsky, L. Kronik, and J. R. Chelikowsky, J. Chem. Phys. **119**, 2284 (2003).

[25] N. T. Maitra, J. Chem. Phys. **122**, 234104 (2005).

[26] J. Andzelm, A. M. Rawlett, J. A. Orlicki, and J. F. Snyder, J. Chem. Theory Comput. **3**, 870 (2007).

[27] N. Govind, M. Valiev, L. Jensen, and K. Kowalski, J. Phys. Chem. A **113**, 6041 (2009).

[28] M. J. G. Peach, C. R. Le Sueur, K. Ruud, M. Guillaume, and D. J. Tozer, Phys. Chem. Chem. Phys. **11**, 4465 (2009).

[29] N. Kuritz, T. Stein, R. Baer, and L. Kronik, J. Chem. Theory Comput. **7**, 2408 (2011).

[30] M. J. G. Peach, M. J. Williamson, and D. J. Tozer, J. Chem. Theory Comput. **7**, 3578 (2011).

[31] M. Srebro, N. Govind, W. A. de Jong, and J. Autschbach, J. Phys. Chem. A **115**, 10930 (2011).

[32] R. M. Richard and J. M. Herbert, J. Chem. Theory Comput. **7**, 1296 (2011).

[33] A. Chantzis, A. D. Laurent, C. Adamo, and D. Jacquemin, J. Chem. Theory Comput. **9**, 4517 (2013).

[34] R. Bauernschmitt, M. Haser, O. Treutler, and R. Ahlrichs, Chem. Phys. Lett. **264**, 573 (1997).

[35] J. R. Chelikowsky, L. Kronik, and I. Vasiliev, J. Phys.: Condens. Matter **15**, R1517 (2003).

[36] J. Gavnholt, A. Rubio, T. Olsen, K. S. Thygesen, and J. Schiotz, Phys. Rev. B **79**, 195405 (2009).

[37] S. Hirata and M. Head-Gordon, Chem. Phys. Lett. **302**, 375 (1999).

[38] S. Hirata, T. J. Lee, and M. Head-Gordon, J. Chem. Phys. **111**, 8904 (1999).

[39] D. Jacquemin, E. A. Perpete, G. E. Scuseria, I. Ciofini, and C. Adamo, J. Chem. Theory Comput. **4**, 123 (2008).

[40] T. Stein, L. Kronik, and R. Baer, J. Chem. Phys. **131**, 244119 (2009).

[41] T. Stein, L. Kronik, and R. Baer, J. Am. Chem. Soc. **131**, 2818 (2009).

[42] H. Phillips, S. Zheng, A. Hyla, R. Laine, T. Goodson, E. Geva, and B. D. Dunietz, J. Phys. Chem. A **116**, 1137 (2011).

[43] Q. Ou, S. Fatehi, E. Alguire, Y. Shao, and J. E. Subotnik, J. Chem. Phys. **141**, 024114 (2014).

[44] M. Parac and S. Grimme, Chem. Phys. **292**, 11 (2003).

[45] S. Grimme and M. Parac, ChemPhysChem **4**, 292 (2003).

[46] A. Dreuw and M. Head-Gordon, J. Am. Chem. Soc. **126**, 4007 (2004).

[47] N. T. Maitra, F. Zhang, R. J. Cave, and K. Burke, J. Chem. Phys. **120**, 5932 (2004).

[48] W. Hieringer and A. Görling, Chem. Phys. Lett. **419**, 557 (2006).

[49] B. G. Levine, C. Ko, J. Quenneville, and T. J. Martinez, Mol. Phys. **104**, 1039 (2006).

[50] K. Lopata, R. Reslan, M. Kowaska, D. Neuhauser, N. Govind, and K. Kowalski, J. Chem. Theory Comput. **7**, 3686 (2011).

[51] T. Kowalczyk, S. R. Yost, and T. Van Voorhis, J. Chem. Phys. **134**, 054128 (2011).

[52] C. M. Isborn, B. D. Mar, B. F. Curchod, I. Tavernelli, and T. J. Martínez, J. Phys. Chem. B **117**, 12189 (2013).

[53] S. Albrecht, L. Reining, R. Del Sole, and G. Onida, Phys. Rev. Lett. **80**, 4510 (1998).

[54] M. Rohlfing and S. G. Louie, Phys. Rev. B **62**, 4927 (2000).

[55] F. Sottile, M. Marsili, V. Olevano, and L. Reining, Phys. Rev. B **76**, 161103 (2007).

[56] L. E. Ramos, J. Paier, G. Kresse, and F. Bechstedt, Phys. Rev. B **78**, 195423 (2008).

[57] D. Rocca, Y. Ping, R. Gebauer, and G. Galli, Phys. Rev. B **85**, 045116 (2012).

[58] L. Hedin, Phys. Rev. **139**, A796 (1965).

[59] E. E. Salpeter and H. A. Bethe, Phys. Rev. **84**, 1232 (1951).

[60] M. S. Hybertsen and S. G. Louie, Phys. Rev. Lett. **55**, 1418 (1985).

[61] M. S. Hybertsen and S. G. Louie, Phys. Rev. B **34**, 5390 (1986).

[62] L. Steinbeck, A. Rubio, L. Reining, M. Torrent, I. White, and R. Godby, Comput. Phys. Commun. **125**, 105 (2000).

[63] M. M. Rieger, L. Steinbeck, I. White, H. Rojas, and R. Godby, Comput. Phys. Commun. **117**, 211 (1999).

[64] P. Rinke, A. Qteish, J. Neugebauer, C. Freysoldt, and M. Scheffler, New J. Phys. **7**, 126 (2005).

[65] J. B. Neaton, M. S. Hybertsen, and S. G. Louie, Phys. Rev. Lett. **97**, 216405 (2006).

[66] M. L. Tiago and J. R. Chelikowsky, Phys. Rev. B **73**, 205334 (2006).

[67] C. Friedrich and A. Schindlmayr, NIC Ser. **31**, 335 (2006).

[68] M. Gruning, A. Marini, and A. Rubio, J. Chem. Phys. **124**, 154108 (2006).

[69] M. Shishkin and G. Kresse, Phys. Rev. B **75**, 235102 (2007).

[70] P. Huang and E. A. Carter, Annu. Rev. Phys. Chem. **59**, 261 (2008).
[71] C. Rostgaard, K. W. Jacobsen, and K. S. Thygesen, Phys. Rev. B **81**, 085103 (2010).
[72] I. Tamblyn, P. Darancet, S. Y. Quek, S. A. Bonev, and J. B. Neaton, Phys. Rev. B **84**, 201402 (2011).
[73] P. Liao and E. A. Carter, Phys. Chem. Chem. Phys. **13**, 15189 (2011).
[74] S. Refaely-Abramson, R. Baer, and L. Kronik, Phys. Rev. B **84**, 075144 (2011).
[75] N. Marom, F. Caruso, X. Ren, O. T. Hofmann, T. Körzdörfer, J. R. Chelikowsky, A. Rubio, M. Scheffler, and P. Rinke, Phys. Rev. B **86**, 245127 (2012).
[76] L. Y. Isseroff and E. A. Carter, Phys. Rev. B **85**, 235142 (2012).
[77] S. Refaely-Abramson, S. Sharifzadeh, N. Govind, J. Autschbach, J. B. Neaton, R. Baer, and L. Kronik, Phys. Rev. Lett. **109**, 226405 (2012).
[78] L. Kronik, T. Stein, S. Refaely-Abramson, and R. Baer, J. Chem. Theory Comput. **8**, 1515 (2012).
[79] L. X. Benedict, E. L. Shirley, and R. B. Bohn, Phys. Rev. Lett. **80**, 4514 (1998).
[80] L. X. Benedict, A. Puzder, A. J. Williamson, J. C. Grossman, G. Galli, J. E. Klepeis, J.-Y. Raty, and O. Pankratov, Phys. Rev. B **68**, 085310 (2003).
[81] C. D. Spataru, S. Ismail-Beigi, L. X. Benedict, and S. G. Louie, Phys. Rev. Lett. **92**, 077402 (2004).
[82] N. Sai, M. L. Tiago, J. R. Chelikowsky, and F. A. Reboredo, Phys. Rev. B **77**, 161306 (2008).
[83] F. Fuchs, C. Rödl, A. Schleife, and F. Bechstedt, Phys. Rev. B **78**, 085103 (2008).
[84] M. Palummo, C. Hogan, F. Sottile, P. Bagala, and A. Rubio, J. Chem. Phys. **131**, 084102 (2009).
[85] L. Schimka, J. Harl, A. Stroppa, A. Gruneis, M. Marsman, F. Mittendorfer, and G. Kresse, Nat. Mater. **9**, 741 (2010).
[86] D. Rocca, D. Lu, and G. Galli, J. Chem. Phys. **133**, 164109 (2010).
[87] X. Blase and C. Attaccalite, Appl. Phys. Lett. **99**, 171909 (2011).
[88] C. Faber, I. Duchemin, T. Deutsch, C. Attaccalite, V. Olevano, and X. Blase, J. Mater. Sci. **47**, 7472 (2012).
[89] C. Faber, P. Boulanger, C. Attaccalite, I. Duchemin, and X. Blase, Philos. Trans. A Math. Phys. Eng. Sci. **372**, 20130271 (2014).
[90] B. Walker, A. M. Saitta, R. Gebauer, and S. Baroni, Phys. Rev. Lett. **96**, 113001 (2006).
[91] D. Rocca, R. Gebauer, Y. Saad, and S. Baroni, J. Chem. Phys. **128**, 154105 (2008).
[92] H. F. Wilson, F. Gygi, and G. Galli, Phys. Rev. B **78**, 113303 (2008).
[93] S. Baroni, S. de Gironcoli, A. Dal Corso, and P. Giannozzi, Rev. Mod. Phys. **73**, 515 (2001).
[94] R. Baer, D. Neuhauser, and E. Rabani, Phys. Rev. Lett. **111**, 106402 (2013).
[95] D. Neuhauser, R. Baer, and E. Rabani, J. Chem. Phys. **141**, 041102 (2014).
[96] D. Neuhauser, E. Rabani, and R. Baer, J. Chem. Theory Comput. **9**, 24 (2013).
[97] Q. Ge, Y. Gao, R. Baer, E. Rabani, and D. Neuhauser, J. Phys. Chem. Lett. **5**, 185 (2013).
[98] D. Neuhauser, E. Rabani, and R. Baer, J. Phys. Chem. Lett. **4**, 1172 (2013).
[99] R. Baer and E. Rabani, Nano Lett. **12**, 2123 (2012).
[100] D. Neuhauser, Y. Gao, C. Arntsen, C. Karshenas, E. Rabani, and R. Baer, Phys. Rev. Lett. **113**, 076402 (2014).
[101] Y. Gao, D. Neuhauser, R. Baer, and E. Rabani, J. Chem. Phys. **142**, 034106 (2015).
[102] M. E. Casida, Recent Adv. Comp. Chem. **1**, 155 (1995).
[103] M. E. Casida, in *Recent Developments and Applications in Density Functional Theory*, edited by J. M. Seminario (Elsevier, Amsterdam, 1996), pp. 391–439.
[104] F. Furche, Phys. Rev. B **64**, 195120 (2001).
[105] F. J. Dyson, Phys. Rev. **90**, 994 (1953).
[106] J. Taylor, Phys. Rev. **95**, 1313 (1954).
[107] S. Hirata and M. Head-Gordon, Chem. Phys. Lett. **314**, 291 (1999).
[108] S. Hirata, M. Head-Gordon, and R. J. Bartlett, J. Chem. Phys. **111**, 10774 (1999).
[109] R. Baer and D. Neuhauser, Phys. Rev. Lett. **94**, 043002 (2005).
[110] E. N. Brothers, A. F. Izmaylov, J. O. Normand, V. Barone, and G. E. Scuseria, J. Chem. Phys. **129**, 011102 (2008).
[111] L. W. Wang and A. Zunger, J. Phys. Chem. **98**, 2158 (1994).
[112] L. W. Wang and A. Zunger, Phys. Rev. B **51**, 17398 (1995).
[113] L. W. Wang and A. Zunger, Phys. Rev. B **53**, 9579 (1996).
[114] H. Fu and A. Zunger, Phys. Rev. B **55**, 1642 (1997).
[115] A. J. Williamson and A. Zunger, Phys. Rev. B **61**, 1978 (2000).
[116] A. Franceschetti and A. Zunger, Phys. Rev. B **62**, 2614 (2000).
[117] A. Zunger, Phys. Status Solidi B **224**, 727 (2001).
[118] H. X. Fu and A. Zunger, Phys. Rev. B **56**, 1496 (1997).
[119] E. Rabani, B. Hetenyi, B. J. Berne, and L. E. Brus, J. Chem. Phys. **110**, 5355 (1999).
[120] F. A. Reboredo, A. Franceschetti, and A. Zunger, Phys. Rev. B **61**, 13073 (2000).
[121] A. Franceschetti and A. Zunger, Phys. Rev. B **62**, R16287 (2000).
[122] H. Eshet, M. Grünwald, and E. Rabani, Nano Lett. **13**, 5880 (2013).
[123] L. W. Wang and A. Zunger, Phys. Rev. Lett. **73**, 1039 (1994).
[124] A. Zunger and L. W. Wang, Appl. Surf. Sci. **102**, 350 (1996).
[125] R. Kosloff, J. Phys. Chem. **92**, 2087 (1988).